Journal of Thermal Analysis and Calorimetry (2020) 140:309–319
https://doi.org/10.1007/s10973-019-08775-8

Performance enhancement of a humidification–dehumidification desalination system

A thermodynamic investigation

Iskander Tlili[1,2] · M. Osman[3,4] · E. M. Barhoumi[5,6] · I. Alarifi[3] · Ahmed G. Abo-Khalil[7,8] · R. P. Praveen[7] · Khairy Sayed[9]

Received: 11 July 2019 / Accepted: 30 August 2019 / Published online: 16 September 2019

Abstract

The purpose of the present work is to investigate humidification–dehumidification desalination system and to explore the effect of pertinent parameters on the overall performance of the process taking in account the irreversibilities and energy losses. The system has been inspected using first and second laws of thermodynamics, and an optimization of the performance along with design development has been performed based on mathematical calculation and modeling for the fundamental equations associated with mass, energy, exergy and salinity balance incorporating the effects of irreversibilities and thermal losses which in turn helps in establishing an efficient desalination system by reducing these losses. The results show a good improvement compared to previous studies. The model target is to increase heat exchange in humidifier and dehumidifier compartment as well as augmenting pure water capacity and lessening energy consumption. Results expose that the inlet water temperature and flow rate represent the main factors affecting the system performance. It is found that the heater has the main part of exergy losses. Increasing the temperature of the water in the dehumidifier outlet allows minimizing the exergy losses in the dehumidifier.

Keywords Humidification–dehumidification · Mathematical programming · Optimization · Irreversibilities · Performance · Design

List of symbols

A	Area (m^2)
a	Specific area (m^2/m^3)
C_p	Specific heat at constant pressure ($Jkg^{-1}\ K^{-1}$)
C_v	Specific heat at constant volume ($Jkg^{-1}\ K^{-1}$)
H	Enthalpy ($kJ\ kg^{-1}$)

✉ Ahmed G. Abo-Khalil
a.abokhalil@mu.edu.sa

1 Department for Management of Science and Technology Development, Ton Duc Thang University, Ho Chi Minh City, Vietnam

2 Faculty of Applied Sciences, Ton Duc Thang University, Ho Chi Minh City, Vietnam

3 Department of Mechanical and Industrial Engineering, College of Engineering, Majmaah University, Majmaah 11952, Kingdom of Saudi Arabia

4 Mechanical Design Department, Faculty of Engineering Mataria, Helwan University, Cairo El-Mataria 11724, Egypt

5 Department of Electrical and Computer Engineering, College of Engineering, Dhofar University, Salalah, Oman

6 Laboratoire Analyse, Conception et Commande des Systèmes (LR11ES20), Ecole Nationale d'Ingénieurs de Tunis, Université de Tunis El Manar, Tunis, Tunisia

7 Department of Electrical Engineering, College of Engineering, Majmaah University, Almajmaah 11952, Saudi Arabia

8 Department of Electrical Engineering, College of Engineering, Assuit University, Assuit 71515, Egypt

9 Electrical Engineering Department, College of Engineering, Sohag University, Sohag 82524, Egypt

h	Heat transfer coefficient (W m^{-2} K^{-1})
k	Mass transfer coefficient (kg m^{-2} S^{-1})
$\dot{m}$	Mass flow rate (kg s^{-1})
N	Mole fraction
Q_L	Latent heat evaporation (J kg^{-1})
$\dot{Q}$	Heat flux (kW)
T	Temperature (°C)
P	Pressure (kPa)
$\dot{S}_{gen}$	Rate of entropy generation (J K^{-1})
X	Salt concentration (TDS)
z	Elevation (m)
ε	Heat exchanger efficiency

Subscripts

a	Air
con	Condenser
e	Evaporator
f	Feed water
hex	Heat exchanger
in	Inlet
out	Outlet
pur	Pure water
bra	Brackish water
s	Salt
vap	Vapor
i	Interface
m	Mass
n	Number of effect
Loss	Losses
w	Water

Introduction

Desalination systems are widely used in several industries, and the multi-effect distillation MED and multi-stage MS used to investigate the thermodynamic application of second law could lead to improving the performance of processes. Designers and engineers extract from thermodynamic laws to find out the exergy analysis. The motivation behind this research work is because potable water is becoming more scarce, which means it is imperative to find solutions to better manage and produce clean water at low cost. The second motivation is that water desalination processes involve huge amounts of energy and the reduction in thermal consumption, along with higher performance representing a challenge for many engineers and researchers.

The humidification–dehumidification desalination system is a promising process technology that is combined with solar energy for small production plants. The most recent studies have discussed ways to improve the distillate production and enhance the desalination system's performance. The novelty of the present study is that it can be compared with recently published research, as the purpose of this study is to design and optimize a humidifier–dehumidifier desalination system with higher performance and lower energy consumption, and that could run on solar energy.

The present research approach involves several researchers treating the humidifier–dehumidifier desalination system from different perspectives; however, to the authors' best knowledge, no previous studies have included both irreversibilities, exergy and heat losses through main compartments, and the results obtained in this study are the closest to experimentally when compared to other studies.

System productivity is mostly influenced by the airflow rate and water temperature, although a minor influence is from the level of water. The humidifier's productivity and the desalination system's thermal productivity are aimed at maximum efficiency [1]. Humidification–dehumidification (HD) desalination cycles have been used to define in what way cycles and mechanisms can be enhanced. It has been found that the cycle minimized specific entropy generation and then increased the output ratio (GOR) [2]. Muthusamy et al. observed that the energy and exergy analysis construed the energy's effective utilization quantity with the changed HDH desalination system. The improved system resulted in a 45% productivity enhancement when compared to a 0.340 kg h^{-1} conventional system [3].

Humidification–dehumidification (HD) desalination system's productivity improved by modifying the behavior of the flow in its mechanisms using a modern type of insertion for supplements and packing material; this was performed with two different types of humidifier [4]. This study's results show that the system yield was maximized, with a maximized flow rate for water and air [5]. This study's results show that this component has good productivity and performance because of the latent heat re-utilization of vapor condensation between the two system loops during desalination [5]. Xu et al. compared the performance between open/close cycles and found that the open cycle yielded the most, with a cooling seawater flow rate increase, which differed to that of the closed cycle [6].

He et al. detected that a minor temperature difference of a lower value for the condenser produced higher values both for humidification and dehumidification and was effective in examining the production of water and the consistent efficiency of the thermal system [7–12]. Saeed et al. applied a mathematical model and examined the system's performance under different working conditions, including the humidifier and dehumidifier's efficiency through theoretical modeling [13]. They proposed a model using a mathematical system that is more effective for forecasting distillate production than the existing research results at preserving sensible temperature calculations [14–18].

Sharshir et al. used a theoretical model to compare the average hourly fresh water accumulative variations in productivity from 9 a.m. to 5 p.m. It is initiated that the accumulated distillate amount for wick solar still with and without film cooling is maximum than that of predictable solar remain continuously, where the typical every hour freshwater productivity is maximum for wick remain with and without mat cooling [19]. This theoretical study is in agreement with the experimental data, with the highest percentage deviation at 5% from the investigational data, and the cycle of improved obtained approximately 100% improvement in the performance of energy completed the basic cycle because with heat process recovery connected with the cycle of improvement [20–23].

Huifang et al. compared with the existing multi-effect humidification–dehumidification desalination system, it recycles the concentration the heat of latent and recycles the heat of residual in the saline successfully [24]. The numerical model is applied to examine the performance of this installation type exposed to the control parameters differences [25]. HDH desalination process is a promising system for producing new water to meet limited water demand. In general, thermal energy required to run the HDH system can be found from the sources of renewable similar the geothermal energy and solar permit temperature process performed [26, 27]. The maximum change in the enthalpy rates of either stream exchanging energy is equivalent and characterizes the balancing in the thermal state for an immediate mass exchange and heat system [28]. The mass rate ratio studies the effect on the fixed-size system performance, and they study its conclusion on the generation of entropy and the driving forces for heat and mass transfer. Likewise, they describe energy effectiveness generalized for mass exchangers and the temperature [29–38].

The desalination system operation is consuming the highest performance after the heat rate ratio roughly reaches value one. In this situation only, the water source one is heated, if the Intel of energy is minimum, the heating of water is a much good result for an effective system, nevertheless after the heat inlet is maximum; the heating of air is further operative [39–49]. Humidification–dehumidification desalination process with the double-stages solar multi-effect has maximum energy improvement rate than the single-phase preforms [50–56]. Recovery ratio congregates to determine as the extractions/injections number upsurges and the closed loop-air model, HDH open loop-water systems with the extractions/injections of the air, the rate ratio of the mass flow variations because of condensation and evaporation within a single stage can be avoided [57–66]. In this present research work, the authors provide the best solution to some existing problems with the humidifier–dehumidifier desalination system with higher performance and lower energy consumption that lead to save some energy and reduce the pollution in the environment. Compared to previous published works, the improved humidification–dehumidification model taking into account energy losses and irreversibility has been developed and studied in this paper.

Mathematical formulation

The proposed model of the humidification–dehumidification system incorporates three major compartments which are heater, humidifier and dehumidifier as exposed in Fig. 1. The humidification–dehumidification system is characterized by two types of flow with open or closed air cycle. Some researchers [8–15] reported that thermal efficiency increases and reaches in case of closed air cycle; however, in case of open air cycle, pure water production augments meaningfully. In the dehumidifier section, the vapor or the humid air produced in the humidifier will be condensed in contact with cooled surface which led to produce pure water, and the feed water temperature will increase by latent heat of condensation in the dehumidifier section. While in the humidifier section, amount of vapor will be removed by air. Finally, heater supply air or water or both of them with amount of heat.

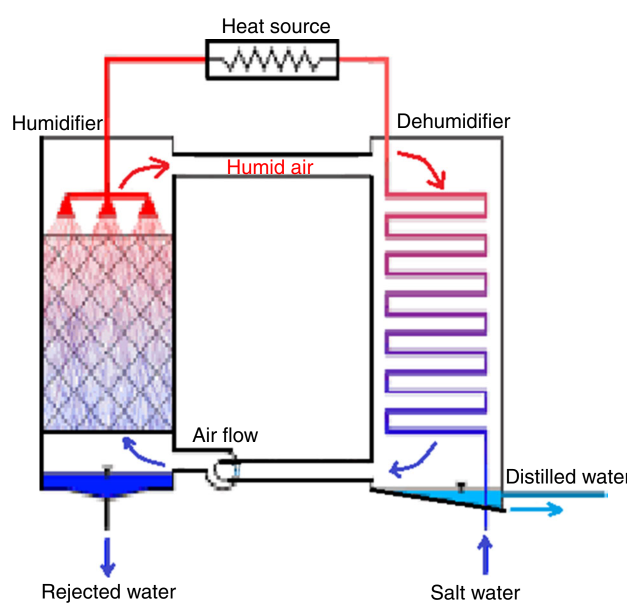

Fig. 1 Humidification–dehumidification desalination system configuration

The established mathematical model based on the models of the components led to governing equations related to mass, energy and exergy balance which are used to define the rate of heat transfer and heat balance in three all major section humidifier, dehumidifier and heater according the following assumption:

- Steady state natural air flow.
- Water distribution over the humidifier is uniform.
- Gradient of humidity and temperature is vertical in both humidifier and dehumidifier.
- Humid air is considered as gas perfect.
- The mathematical model considers atmospheric pressure.
- Kinetic and potential energy variations were neglected.

Figure 2a–c illustrates the control volume in all three part water, interface and humid air.

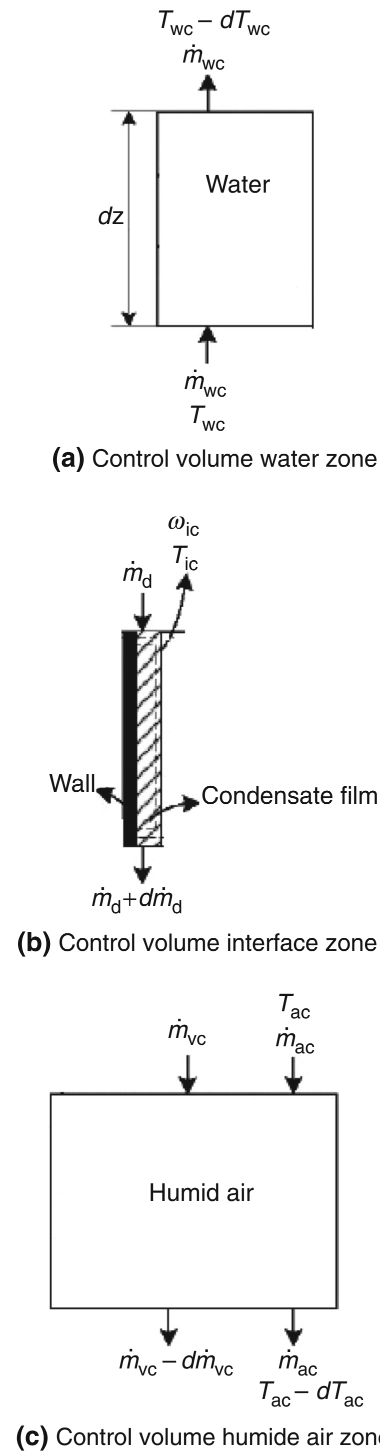

Fig. 2 **a** Control volume water zone, **b** control volume interface zone, **c** control volume humide air zone

Exergy losses

Bejan [47] established the Standard chemical exergy of ideal gas mixture which is defined by:

$$e^{-\mathrm{CH}} = \sum^{n} x_k e_k^{-\mathrm{CH}} + RT_0 \sum \ln N_k \tag{1}$$

where N_k represent the mole fraction.

Exergy losses due to mass transfer are defined by:

$$\mathrm{EX}_{\mathrm{Loss,m}} = \mathrm{EX}_{\mathrm{in}} - \mathrm{EX}_{\mathrm{out}} \tag{2}$$

The following equation gives input and output exergy,

$$\begin{aligned}\mathrm{EX}_{\mathrm{in}} &= \mathrm{RT}_0[n_{\mathrm{Ai}}\mathrm{Ln}(N_{\mathrm{Ai}}) + n_{\mathrm{Bi}}\mathrm{Ln}(N_{\mathrm{Bi}})]\\ &= \mathrm{RT}_0\mathrm{Ln}\left(N_{\mathrm{Ai}}^{\mathrm{n_{Ai}}} \times N_{\mathrm{Bi}}^{\mathrm{n_{Bi}}}\right)\end{aligned} \tag{3}$$

$$\begin{aligned}\mathrm{EX}_{\mathrm{out}} &= \mathrm{RT}_0[n_{\mathrm{Ae}}\mathrm{Ln}(N_{\mathrm{Ae}}) + n_{\mathrm{Be}}\mathrm{Ln}(N_{\mathrm{Be}})]\\ &= RT_0\mathrm{Ln}\left(N_{\mathrm{Ae}}^{\mathrm{n_{Ae}}} \times N_{\mathrm{Be}}^{\mathrm{n_{Be}}}\right)\end{aligned} \tag{4}$$

Therefore, the exergy losses due to concentration change are presented below by:

$$\mathrm{EX}_{\mathrm{Loss}} = \mathrm{RT}_0\mathrm{Ln}\left(\frac{N_{\mathrm{Ai}}^{\mathrm{n_{Ai}}} \times N_{\mathrm{Bi}}^{\mathrm{n_{Bi}}}}{N_{\mathrm{Ae}}^{\mathrm{n_{Ae}}} \times N_{\mathrm{Be}}^{\mathrm{n_{Be}}}}\right) \tag{5}$$

The second law of thermodynamics proves that the greater temperature heat sources cannot transfer all the entire heat to the lesser temperature heat source; therefore, exergy losses appear in this transfer of heat and expressed as follows:

$$\mathrm{EX}_{\mathrm{Loss}_{\Delta T}} = \Delta\mathrm{EX}_{\mathrm{source}_{\Delta T}} - \Delta\mathrm{EX}_{\sin\mathrm{k}_{\Delta T}} \tag{6}$$

The minor and greater temperature heat sources are, respectively, exergy sink and source.

Where $\Delta\mathrm{EX}_{\sin\mathrm{k}_{\Delta T}}$ and $\Delta\mathrm{EX}_{\mathrm{source}_{\Delta T}}$ represent, respectively, the sink and source exergy variation.

Consider, the environment temperature T_0, exergy source temperature is T_1, the exergy sink temperature is T_2 and the heat transfer rate among them are $\dot{q}$; therefore, the exergy variation for sink and source is, respectively

$$\Delta \mathrm{EX}_{\mathrm{sink}_{\Delta T}} = \dot{q}\left(1 - \frac{T_0}{T_2}\right) \tag{7}$$

$$\Delta \mathrm{EX}_{\mathrm{source}_{\Delta T}} = \dot{q}\left(1 - \frac{T_0}{T_1}\right) \tag{8}$$

Consequently, an exergy loss due to temperature variation is defined as follows:

$$\mathrm{EL}_{\Delta \mathrm{T}} = \dot{q}T_0\left(\frac{T_1 - T_2}{T_1 T_2}\right) \tag{9}$$

Finally, the total energy variation due to both mass and heat transfer is:

$$\Delta \mathrm{EX}_{\Delta \mathrm{C},\Delta \mathrm{T}} = (\Delta \mathrm{EX}_{\Delta \mathrm{T}})_{\Delta \mathrm{C}=0} + (\Delta \mathrm{EX}_{\Delta \mathrm{C}})_{\Delta \mathrm{T}=0} \tag{10}$$

To conclude the total exergy losses for humidification–dehumidification system is as follow

$$E_{\mathrm{Loss,total}} = E_{\mathrm{Loss,H}} + E_{\mathrm{Loss,D}} + E_{\mathrm{Loss,HE}} \tag{11}$$

where $E_{\mathrm{Loss,H}}$ is the humidifier exergy losses, $E_{\mathrm{Loss,DH}}$ is the dehumidifier exergy losses and $E_{\mathrm{Loss,HE}}$ is the dehumidifier exergy losses.

Energy analysis

The application of mass balance for the control volume exposed in Fig. 2 can be presented as follows:

$$d\dot{m}_{\mathrm{we}} = d\dot{m}_{\mathrm{ve}} = \dot{m}_{\mathrm{ae}} d\omega_{\mathrm{e}} \tag{12}$$

The heat balance for the same control volume concerning water area

$$\frac{\mathrm{d}T_{\mathrm{we}}}{\mathrm{d}z} = \frac{h_{\mathrm{we}} a_{\mathrm{He}} (T_{\mathrm{we}} - T_{\mathrm{ie}})}{\dot{m}_{\mathrm{we}} C_{\mathrm{we}}} \tag{13}$$

However, for the air region, both mass and heat balance are presented, respectively, as follows:

$$\frac{\mathrm{d}\omega_{\mathrm{e}}}{\mathrm{d}z} = \frac{k_{\mathrm{ae}} a_{\mathrm{Me}} (\omega_{\mathrm{ie}} - \omega_{\mathrm{e}})}{\dot{m}_{\mathrm{ae}}} \tag{14}$$

$$\frac{\mathrm{d}T_{\mathrm{ae}}}{\mathrm{d}z} = \frac{h_{\mathrm{ae}} a_{\mathrm{He}} (T_{\mathrm{ie}} - T_{\mathrm{ae}})}{\dot{m}_{\mathrm{ac}} (C_{\mathrm{ae}} + \omega_{\mathrm{e}} C_{\mathrm{ve}})} \tag{15}$$

Finally, the heat balance for border is presented:

$$\begin{aligned} H_{\mathrm{we}} a_{\mathrm{He}} (T_{\mathrm{we}} - T_{\mathrm{ie}}) \mathrm{d}z = {} & h_{\mathrm{ac}} a_{\mathrm{He}} (T_{\mathrm{ie}} - T_{\mathrm{ae}}) \mathrm{d}z \\ & + L_{\mathrm{ve}} k_{\mathrm{ac}} a_{\mathrm{Mc}} (\omega_{\mathrm{ie}} - \omega_{\mathrm{c}}) \mathrm{d}z \end{aligned} \tag{16}$$

The interface is considered a layer of saturated air; consequently, the absolute humidity $\omega_{\mathrm{int,H}}$ depends on interface temperature $T_{\mathrm{int,H}}$. An experimental research [ ] presents this relation as follows:

$$\begin{aligned} \omega_{\mathrm{ie}} & = f_{\exp}(T_{\mathrm{ie}}) \\ & = 2.19 \times 10^{(-6)} T_{\mathrm{ie}}^3 - 1.85 \times 10^{(-4)} T_{\mathrm{ie}}^2 + 7.06 \\ & \quad \times 10^{(-3)} T_{\mathrm{ie}}^3 - 0.077 \end{aligned} \tag{17}$$

In the second main part related to dehumidifier (Condenser).

The main equations applied to the dehumidifier and consider the same assumption as humidifier.

The application of mass balance for the control volume exposed in Fig. 2 can presented as follows:

$$\mathrm{d}\dot{m}_{\mathrm{d}} = d\dot{m}_{\mathrm{vc}} = \dot{m}_{\mathrm{ac}} d\omega_{\mathrm{c}} \tag{18}$$

The heat balance for the same control volume concerning water section

$$\frac{\mathrm{d}T_{\mathrm{wc}}}{\mathrm{d}z} = \frac{h_{\mathrm{wc}} a_{\mathrm{Hc}} (T_{\mathrm{ic}} - T_{\mathrm{wc}})}{\dot{m}_{\mathrm{wc}} C_{\mathrm{wc}}} \tag{19}$$

However, for the air section, both mass and heat balance are presented, respectively, as follows:

$$\frac{\mathrm{d}\omega_{\mathrm{c}}}{\mathrm{d}z} = \frac{k_{\mathrm{ac}} a_{\mathrm{Mc}} (\omega_{\mathrm{c}} - \omega_{\mathrm{ic}})}{\dot{m}_{\mathrm{ac}}} \tag{20}$$

$$\frac{\mathrm{d}T_{\mathrm{ac}}}{\mathrm{d}z} = \frac{h_{\mathrm{ac}} a_{\mathrm{Hc}} (T_{\mathrm{ac}} - T_{\mathrm{ic}})}{\dot{m}_{\mathrm{ac}} (C_{\mathrm{ac}} + \omega_{\mathrm{c}} C_{\mathrm{vc}})} \tag{21}$$

Finally, the heat balance for the interface is presented:

$$\begin{aligned} H_{\mathrm{wc}} a_{\mathrm{Hc}} (T_{\mathrm{we}} - T_{\mathrm{ic}}) = {} & h_{\mathrm{ac}} a_{\mathrm{Hc}} (T_{\mathrm{ic}} - T_{\mathrm{ac}}) \mathrm{d}z \\ & + L_{\mathrm{vc}} k_{\mathrm{ac}} a_{\mathrm{Mc}} (\omega_{\mathrm{ic}} - \omega_{\mathrm{c}}) \end{aligned} \tag{22}$$

The absolute humidity relation is:

$$\begin{aligned} \omega_{\mathrm{int,deh}} & = f_{\exp}(T_{\mathrm{int,deh}}) \\ & = 2.19 \times 10^{(-6)} T_{\mathrm{int,deh}}^3 - 1.85 \times 10^{(-4)} T_{\mathrm{int,deh}}^2 \\ & \quad + 7.06 \times 10^{(-3)} T_{\mathrm{int.deh}}^3 - 0.077 \end{aligned} \tag{23}$$

The last main part related to heater represents an important section in humidification–dehumidification system which supply water with heat to reach certain temperature required for the humidifier.

The heat rate transfer to water flow rate is given by:

$$\dot{Q} = \dot{m} C_{\mathrm{P}} \Delta T \tag{24}$$

For the optimization of humidification–dehumidification system, the pure water production compared to feed water should be maximized, therefore:

$$\text{Max productivity} = \frac{\dot{m}_{\mathrm{d}}}{\dot{m}_{\mathrm{wc}}} \tag{25}$$

As well as in the dehumidifier, the heat recovery should be maximized therefore:

$$\text{Max HR} = \frac{T_{\mathrm{wc}}(1) - T_{\mathrm{wc(m)}}}{T_{\mathrm{we}}(1) - T_{\mathrm{wc(m)}}} \tag{26}$$

In the other hand, the supplier of specific thermal energy should be minimized and is illustrated by:

$$\text{Min specific energy} = \frac{\dot{Q}}{\dot{m}_d} \quad (27)$$

Result and discussion

The proposed model of desalination system was solved using Matlab Software (R2012b, MathWorks limited, London, UK) to evaluate the performances of the optimized system. The thermal energy consumption versus the fed water mass flow rate and the exergy losses in the three main compartments versus the dehumidifier water outlet were calculated. The obtained results of the optimization of both evaporator and condenser surface's are presented and discussed in this section. As well known, the feed water mass flow rate and the temperature have an important effect on the HD desalination efficiency [16]. The variation of specific thermal energy consumption versus the feed water mass flow rate with $T_{fw} = 25$ °C and $\Delta T_{evp} = \Delta T_{con} = 5$ °C, for the optimized cycle, is presented in Fig. 3. The thermal energy consumption takes its minimum for a feed water mass flow rate of 2 kg/s, when the feed water mass flow is lesser than the finest rate that leads to an exponential augmentation of the thermal energy consumption.

The impact of the temperature of the dehumidifier water outlet on exergy losses in the different compartments of the desalination cycle is shown in Fig. 4. The exergy losses in the heater declined from 3.5 kW for 60 °C to 2.4 kW for 68 °C. Increasing the temperature of the water in the dehumidifier outlet allows also minimizing the exergy losses in the dehumidifier as shown in Fig. 4. However, the

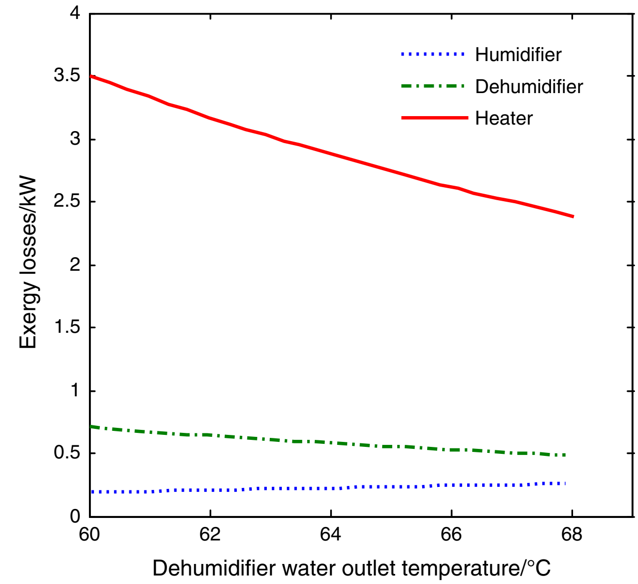

Fig. 4 Dehumidifier water outlet temperature effect on different compartments exergy losses, with $T_{fw} = 25$ °C and $\Delta T_{evp} = \Delta T_{con} = 5$ °C; $\dot{m}_{pw} = 0.005$ kg s^{-1}

exergy losses in the humidifier increase slowly to reach of weak value of 0.22 kW. In overall, the results show an important improvement of desalination process by minimizing the total exergy losses.

The results presented in Fig. 5 show the variation of the gained output ratio (GOR) versus the feed water temperature for different $T_{W;O;H}$. For different values of $T_{W;O;H}$, the GOH is maximum for a temperature of feed water equal to 31.5 °C. Increasing $T_{W;O;H}$ from 80 to 110 °C allows to step up the GOR from 2.9 to 2.97. The presented results

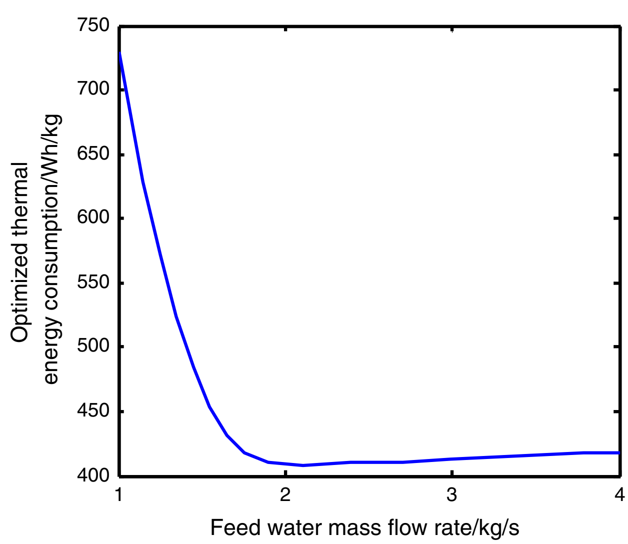

Fig. 3 Variation of specific thermal energy consumption with feed water mass flow rate with $T_{fw} = 25$ °C and $\Delta T_{evp} = \Delta T_{con} = 5$ °C

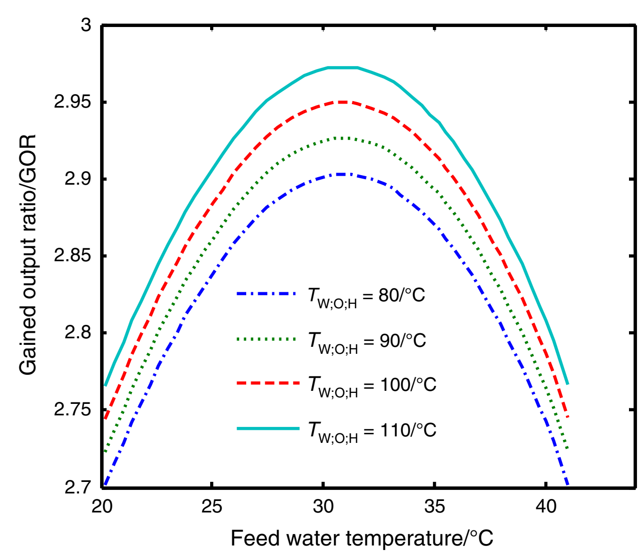

Fig. 5 Effect of feed water temperature on system performance with $T_{fw} = 25$ °C and $\Delta T_{evp} = \Delta T_{con} = 5$ °C; $\dot{m}_{pw} = 0.006$ kg s^{-1}

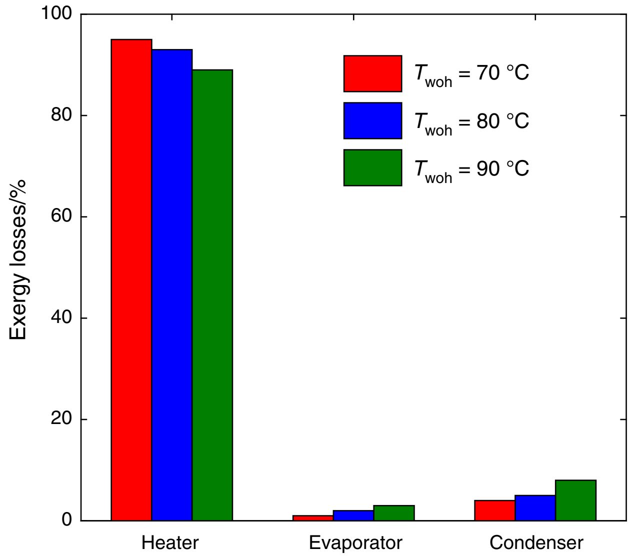

Fig. 6 Exergy losses distribution through three main compartments

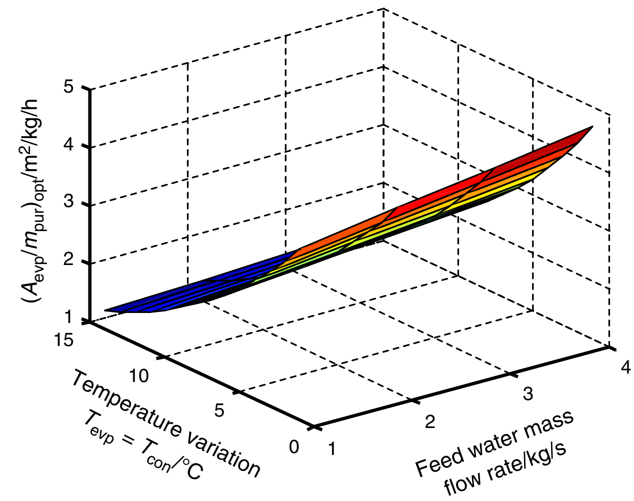

Fig. 8 Optimization of evaporator surface with both feed water mass flow rate and temperature variation in humidifier and dehumidifier

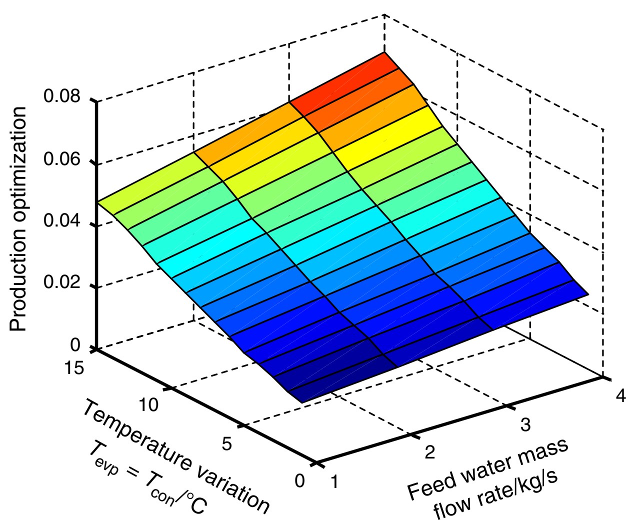

Fig. 7 Effect of feed water mass flow rate and temperature variation in both humidifier and dehumidifier on production optimization

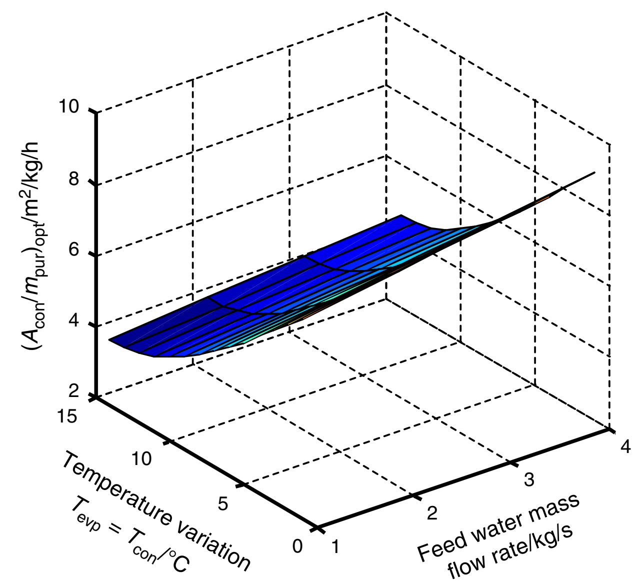

Fig. 9 Optimization of condenser surface with both feed water mass flow rate and temperature variation in humidifier and dehumidifier

show the importance of working at high temperature in aim to increase the GOR.

According to the results shown in Fig. 6, the exergy losses in the heater represent about 95% of the total losses for a temperature of water outlet heater of 70 °C. The losses in the evaporator represent the less part of the total losses. Increasing the temperature allows to minimize the losses in the heater. The histogram shows that the exergy losses in both evaporator and condenser increase with the increasing of the temperature.

The target of the developed model for the HD water desalination process is to increase the production of pure water. The 3D surface shown in Fig. 7 allows to quantify the effect of the temperature variation in the humidifier and the dehumidifier and the feed water mass flow rate on the pure water production. It is clear that increasing temperature or the feed water mass flow rate allows increasing the quantity of produced pure water. The 3D surface shows that the optimum of production is obtained for maximum values of both temperature and feed water mass flow rate.

The new modeling of the enhanced HD water desalination system allows investigating the effect of the temperature variation in the humidifier and the dehumidifier and the feed water mass flow on evaporator surface. The result of Fig. 8 shows that optimum evaporator surface is

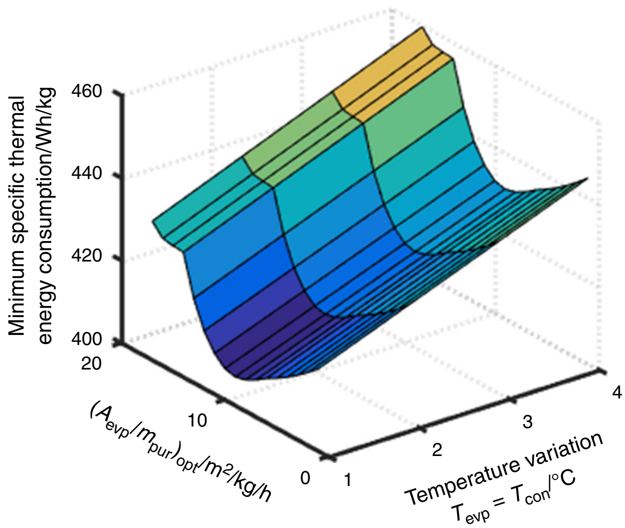

Fig. 10 Minimization of specific thermal energy consumption with both evaporator surface and temperature variation in humidifier and dehumidifier

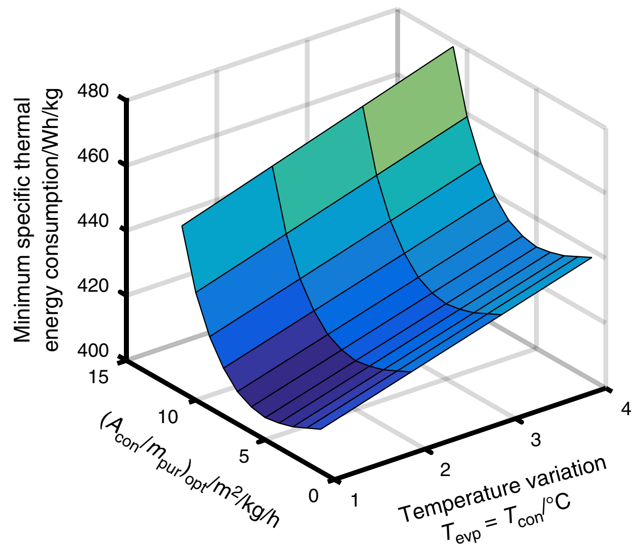

Fig. 11 Minimization of specific thermal energy consumption with both condenser surface and temperature variation in humidifier and dehumidifier

obtained at higher temperature and lower feed water mass flow rate. At the same temperature, increasing the feed water mass flow conducts to a slow increase in the evaporator area. However, the effect of the temperature on the evaporator area is more intense. Indeed, at constant feed water mass flow rate, any variation of temperature is accompanied with strong variation of the evaporator area.

The effect of the temperature variation and feed water mass flow rate on the condenser surface is shown in Fig. 9. The analysis of the 3D surface proves that an optimum (minimum) of the condenser surface of 3.7 $m^2\ kg^{-1}\ h^{-1}$ is obtained for a temperature of 15 °C and a feed water mass flow rate of 1.2 kg s^{-1}. Expanding the feed water mass flow rate for the same temperature corresponds to an increase in the condenser surface. The effect of any variation of the feed water mass flow rate on the condenser surface is stronger for lower temperature values.

The minimization of the specific thermal energy consumption has important consequence of the overall system efficiency. Usually, the objective is to produce the maximum pure water with minimum electrical power consumption. In Fig. 10, it is perceived that the lowest specific thermal energy consumption is achieved at lower temperature variation and for evaporator area of 9.8 m^2/kg/h. According to the presented results, temperature variation of both evaporator and condenser should be kept at minimum values to minimize the specific thermal energy consumption. On the other hand, increasing or decreasing the evaporator area induces an increase in specific thermal energy consumption.

For particular values of condenser surface and temperature variation, the specific thermal energy consumption is minimum. The conducted study analyzes the effect of temperature variation, and the condenser surface is presented in the 3D surface given in Fig. 11. It is clear that the specific energy consumption is minimum for just one couple of condenser area–temperature variation. Increasing the temperature variation increases the specific energy consumption for all values of the condenser area. However, the optimum specific energy consumption is obtained for condenser area equal to 6 (Please check the value and the unit). Increasing or decreasing the condenser area increases the specific thermal energy consumption.

Conclusions

An improved humidification–dehumidification model taking into account energy losses and irreversibility has been developed and studied in this paper. Compared to previous published works, the developed model allows examining effectively the effect of different parameters such as the temperature variation and the feed water mass flow rate on the efficiency of the desalination system. The simulation results presented in the paper showed the efficiency of the optimization of the HD desalination process considering energy losses and irreversibility. Indeed, the results of this investigation are more accurate compared to previous research work.

The new modeling approach leads to the following optimization results:

- Through the new concept of analysis, exergy losses in three main compartments of HD desalination system can be calculated separately. The results show that the heater has the main part of exergy losses. Increasing the temperature of the water in the dehumidifier outlet allows minimizing the exergy losses in the dehumidifier.
- The working at high temperature permits to increase the GOR. The GOR is maximum for a temperature of feed water equal to 31.5 °C. On the other hand, increasing $T_{W;O;H}$ from 80 to 110 °C permits to increase the GOR from 2.9 to 2.97.
- Increasing temperature or the feed water mass flow rate improves the quantity of produced pure water. Pure water optimum production is obtained for maximum values of both temperature and feed water mass flow rate.
- The optimum evaporator surface corresponds to higher water temperature and lower feed water mass flow rate. At the same temperature, increasing the feed water mass flow conducts to a slow increase in the evaporator area. However, at constant feed water mass flow rate, the variation of temperature induces strong variation of the evaporator area.
- For lower temperature variation and for evaporator area of 9.8 $m^2\ kg^{-1}\ h^{-1}$, specific thermal energy consumption is optimum. Temperature variation of both evaporator and condenser should be kept at minimum values to minimize the specific thermal energy consumption.

Acknowledgements The authors extend their appreciation to the Deanship of Scientific Research at Majmaah University for funding this work under Project Number No. (RGP-2019-19).

References

1. El-Agouz SA. A new process of desalination by air passing through seawater based on humidification–dehumidification process. Energy. 2010;35(12):5108–14.
2. Mistry KH, Zubair SM. Effect of entropy generation on the performance of humidification–dehumidification desalination cycles. Int J Therm Sci. 2010;49(9):1837–47.
3. Muthusamy C, Srithar K. Energy and exergy analysis for a humidification–dehumidification desalination system integrated with multiple inserts. Desalination. 2015;367:49–59.
4. Muthusamy C, Srithar K. Energy saving potential in humidification–dehumidification desalination system. Energy. 2017;118:729–41.
5. Chang Z, Zheng H, Yang Y, Su Y, Duan Z. Experimental investigation of a novel multi-effect solar desalination system based on humidification–dehumidification process. Renew Energy. 2014;69:253–9.
6. Xu H, Zhao Y, Jia T, Dai YJ. Experimental investigation on a solar assisted heat pump desalination system with humidification–dehumidification. Desalination. 2018;437:89–99.
7. He WF, Han D, Ji C. Investigation on humidification dehumidification desalination system coupled with heat pump. Desalination. 2018;436:152–60.
8. Narayan GP, Sharqawy MH, Lienhard VJH, Zubair SM. Thermodynamic analysis of humidification dehumidification desalination cycles. Desalination Water Treat. 2010;16:339–53.
9. Tlili Iskander, Hamadneh Nawaf N, Khan Waqar A, Atawneh Samer. Thermodynamic analysis of MHD Couette-Poiseuille flow of water-based nanofluids in a rotating channel with radiation and Hall effects. J Therm Anal Calorim. 2018;132(3):1899–912. https://doi.org/10.1007/s10973-018-7066-5.
10. Nguyen TK, Sheikholeslami M, Jafaryar M, et al. Design of heat exchanger with combined turbulator. J Therm Anal Calorim. 2019. https://doi.org/10.1007/s10973-019-08401-7.
11. Sarafraz MM, Tlili I, Tian Z, et al. Thermal analysis and thermo-hydraulic characteristics of zirconia–water nanofluid under a convective boiling regime. J Therm Anal Calorim. 2019. https://doi.org/10.1007/s10973-019-08435-x.
12. Sarafraz MM, Tian Z, Tlili I, et al. Thermal evaluation of a heat pipe working with n-pentane-acetone and n-pentane-methanol binary mixtures. J Therm Anal Calorim. 2019. https://doi.org/10.1007/s10973-019-08414-2.
13. Dehghani S, Date A, Akbarzadeh A. Performance analysis of a heat pump driven humidification–dehumidification desalination system. Desalination. 2018;445:95–104.
14. de Oliveira Lacerda, Campos B, Souza Oliveira, da Costa A, da Costa Ferreira, Junior E. Performance comparison of different mathematical models in the simulation of a solar desalination by humidification–dehumidification. Desalination. 2018;437:184–94.
15. Ashrafizadeh SA, Amidpour M. Exergy analysis of humidification–dehumidification desalination systems using driving forces concept. Desalination. 2012;285:108–16.
16. Zubair SM, Antar MA, Elmutasim SM, Lawal DU. Performance evaluation of humidification–dehumidification (HDH) desalination systems with and without heat recovery options: an experimental and theoretical investigation. Desalination. 2018;436:161–75.
17. Kang H, Yang Y, Chang Z, Zheng H, Duan Z. Performance of a two-stage multi-effect desalination system based on humidification–dehumidification process. Desalination. 2014;344:339–49.
18. Giwa A, Akther N, Al Housani A, Haris S, Hasan SW. Recent advances in humidification dehumidification (HDH) desalination processes: improved designs and productivity. Renew Sustain Energy Rev. 2016;57:929–44.
19. Sharshir SW, El-Samadony MOA, Peng G, Yang N, Essa FA, Hamed MH, Kabeel AE. Performance enhancement of wick solar still using rejected water from humidification–dehumidification unit and film cooling. Appl Therm Eng. 2016;108:1268–78.
20. Khan MN, Tlili I. Innovative thermodynamic parametric investigation of gas and steam bottoming cycles with heat exchanger and heat recovery steam generator: energy and exergy analysis. Energy Rep. 2018;4:497–506. https://doi.org/10.1016/j.egyr.2018.07.007.
21. Khan MN, Tlili I. New advancement of high performance for a combined cycle power plant: thermodynamic analysis. Case Stud Therm Eng. 2018;12:166–75. https://doi.org/10.1016/j.csite.2018.04.001.
22. Khan MN, Tlili I. Performance enhancement of a combined cycle using heat exchanger bypass control: a thermodynamic investigation. J Clean Prod. 2018;192(10):443–52. https://doi.org/10.1016/j.jclepro.2018.04.272.
23. Afridi MI, Tlili I, Qasim M, Khan I. Nonlinear Rosseland thermal radiation and energy dissipation effects on entropy generation in

CNTs suspended nanofluids flow over a thin needle. Bound Value Prob. 2018. https://doi.org/10.1186/s13661-018-1062-3.
24. Soufari SM, Zamen M, Amidpour M. Performance optimization of the humidification–dehumidification desalination process using mathematical programming. Desalination. 2009;237:305–17.
25. Narayan GP, John MGS, Zubair SM. Thermal design of the humidification dehumidification desalination system: an experimental investigation. Int J Heat Mass Transfer. 2013;58(1–2):740–8.
26. Chehayeb KM, Narayan GP, Zubair SM. Thermodynamic balancing of a fixed-size two-stage humidification dehumidification desalination system. Desalination. 2015;369:125–39.
27. Narayan GP, Chehayeb KM, McGovern RK, Thiel GP, Zubair SM. Thermodynamic balancing of the humidification dehumidification desalination system by mass extraction and injection. Int J Heat Mass Transfer. 2013;57(2):756–70.
28. Ahmed MA, Qasem NA, Zubair SM, Gandhidasan P, Bahaidarah HM. Thermodynamic balancing of the regeneration process in a novel liquid desiccant cooling/desalination system. Energy Convers Manag. 2018;176:86–98.
29. Ali M, Vukovic V, Sheikh NA, Ali HM, Sahir MH. Enhancement and integration of desiccant evaporative cooling system model calibrated and validated under transient operating conditions. Appl Therm Eng. 2015;75:1093–105.
30. Tlili I, Alkanhal TA. Nanotechnology for water purification: electrospun nanofibrous membrane in water and wastewater treatment. J Water Reuse Desalination. 2019. https://doi.org/10.2166/wrd.2019.057.
31. Al-Qawasmi A-R, Tlili I (2018) Energy efficiency audit based on wireless sensor and actor networks: air-conditioning investigation. J Eng, Article ID 3640821, 10 pages. https://doi.org/10.1155/2018/3640821
32. Al-Qawasmi A-R, Tlili I. Energy efficiency and economic impact investigations for air-conditioners using wireless sensing and actuator networks. Energy Rep. 2018;4:478–85. https://doi.org/10.1016/j.egyr.2018.08.001.
33. Tlili I, Khan WA, Khan I. Multiple slips effects on MHD SA-Al2O3 and SA-Cu non-Newtonian nanofluids flow over a stretching cylinder in porous medium with radiation and chemical reaction. Results Phys. 2018;8:213–22. https://doi.org/10.1016/j.rinp.2017.12.013.
34. Ali M, Vukovic V, Sheikh NA, Ali HM. Performance investigation of solid desiccant evaporative cooling system configurations in different climatic zones. Energy Convers Manag. 2015;97:323–39.
35. Guo H, Ali HM, Hassanzadeh A. Simulation study of flat-sheet air gap membrane distillation modules coupled with an evaporative crystallizer for zero liquid discharge water desalination. Appl Therm Eng. 2016;108:486–501.
36. Khan MMA, Ibrahim NI, Mahbubul IM, Ali HM, Saidur R, Al-Sulaiman FA. Evaluation of solar collector designs with integrated latent heat thermal energy storage: a review. Solar Energy. 2018;166:334–50.
37. Sajid MU, Ali HM. Recent advances in application of nanofluids in heat transfer devices: a critical review. Renew Sustain Energy Rev. 2019;103:556–92.
38. Rehman TU, Ali HM, Janjua MM, Sajjad U, Yan WM. A critical review on heat transfer augmentation of phase change materials embedded with porous materials/foams. Int J Heat Mass Transfer. 2019;135:649–73.
39. Ramadan K, Tlili I. Shear work, viscous dissipation and axial conduction effects on microchannel heat transfer with a constant wall temperature. Proc Inst Mech Eng Part C J Mech Eng Sci. 2016;230(14):2496–507. https://doi.org/10.1177/0954406215598799.
40. Ramadan K, Tlili I. A numerical study of the extended Graetz problem in a microchannel with constant wall heat flux: shear work effects on heat transfer. J Mech. 2015;31(6):733–43. https://doi.org/10.1017/jmech.2015.29.
41. Khan WA, Rashad AM, Abdou MMM, Tlili I. Natural bioconvection flow of a nanofluid containing gyrotactic microorganisms about a truncated cone. Eur J Mech B Fluids. 2019;75:133–42. https://doi.org/10.1016/j.euromechflu.2019.01.002.
42. Khan MN, Tlili I, Khan WA. Thermodynamic optimization of new combined gas/steam power cycles with HRSG and heat exchanger. Arab J Sci Eng. 2017;42(11):4547–58. https://doi.org/10.1007/s13369-017-2549-4.
43. Khan MN, Khan WA, Tlili I. Forced convection of nanofluid flow across horizontal elliptical cylinder with constant heat flux boundary condition. J Nanofluids. 2019;8(2):386–93. https://doi.org/10.1166/jon.2019.1583.
44. Babar H, Ali HM. Towards hybrid nanofluids: preparation, thermophysical properties, applications, and challenges. J Mol Liq. 2019;241:598–633.
45. Mahdizade EZ, Ameri M. Thermodynamic investigation of a semi-open air, humidification dehumidification desalination system using air and water heaters. Desalination. 2018;428:182–98.
46. Hou S. Two-stage solar multi-effect humidification dehumidification desalination process plotted from pinch analysis. Desalination. 2008;222(1–3):572–8.
47. Bejan A. Method of entropy generation minimization, or modeling and optimization based on combined heat transfer and thermodynamics. Rev Gen Therm. 1996;35:637–46.
48. Tlili I, Timoumi Y, Ben Nasrallah S. Numerical simulation and losses analysis in a stirling engine. Int J Heat Technol. 2006;24(1):97–105.
49. Tlili I, Timoumi Y, Ben Nasrallah S. Thermodynamic analysis of Stirling heat engine with regenerative losses and internal irreversibilities. Int J Engine Res. 2007;9:45–56.
50. Timoumi Y, Tlili I, Nasrallah SB. Performance optimization of Stirling engines. Renew Energy. 2008;33(9):2134–44.
51. Ahmadi MH, Ahmadi MA, Pourfayaz F, Hosseinzade H, Acıkkalp E, Tlili I, Feidt M. Designing a powered combined Otto and Stirling cycle power plant through multi-objective optimization approach. Renew Sustain Energy Rev. 2016;62:585–95.
52. Tlili I. Renewable energy in Saudi Arabia: current status and future potentials. Environ Dev Sustain. 2015;17(4):859–86.
53. Seyednezhad M, Sheikholeslami M, Ali JA, et al. Nanoparticles for water desalination in solar heat exchanger. J Therm Anal Calorim. 2019. https://doi.org/10.1007/s10973-019-08634-6.
54. Barza A, Shourije SR, Pirouzfar V. Industrial optimization of multi-effect desalination equipment for olefin complex. J Therm Anal Calorim. 2019. https://doi.org/10.1007/s10973-019-08279-5.
55. Rashidi S, Karimi N, Mahian O, et al. A concise review on the role of nanoparticles upon the productivity of solar desalination systems. J Therm Anal Calorim. 2019;135:1145. https://doi.org/10.1007/s10973-018-7500-8.
56. Garg K, Khullar V, Das SK, et al. Parametric study of the energy efficiency of the HDH desalination unit integrated with nanofluid-based solar collector. J Therm Anal Calorim. 2019;135:1465. https://doi.org/10.1007/s10973-018-7547-6.
57. Sa'ed A, Tlili I. Numerical investigation of working fluid effect on stirling engine performance. Int J Therm Environ Eng. 2015;10(1):31–6.
58. Tlili I. Finite time thermodynamic evaluation of endoreversible Stirling heat engine at maximum power conditions. Renew Sustain Energy Rev. 2012;16(4):2234–41.
59. Tlili I. Thermodynamic study on optimal solar stirling engine cycle taking into account the irreversibilities effects. Energy Proc. 2012;14:584–91.

60. Tlili I. A Numerical investigation of an alpha stirling engine using the Ross Yoke linkage. J Heat Technol. 2012;30:23–36.
61. Tlili I, Sa'ed A. Thermodynamic evaluation of a second order simulation for Yoke Ross Stirling engine. Energy Convers Manag. 2013;68:149–60.
62. Tlili I, Timoumi Y, Nasrallah SB. Analysis and design consideration of mean temperature differential Stirling engine for solar application. Renew Energy. 2008;33:1911–21.
63. Tlili I, Khan WA, Ramadan K. MHD flow of nanofluid flow across horizontal circular cylinder: steady forced convection. J Nanofluids. 2019;8(1):179–86. https://doi.org/10.1166/jon.2019.1574.
64. Tlili I, Khan WA, Ramadan K. Entropy generation due to MHD stagnation point flow of a nanofluid on a stretching surface in the presence of radiation. J Nanofluids. 2018;7(5):879–90. https://doi.org/10.1166/jon.2018.1513.
65. Almutairi MM, Osman M, Tlili I. Thermal behavior of auxetic honeycomb structure: an experimental and modeling investigation. ASME J Energy Resour Technol. 2018;140(12):122904–122904-8. https://doi.org/10.1115/1.4041091.
66. Tlili I, Hamadneh NN, Khan WA. Thermodynamic analysis of MHD heat and mass transfer of nanofluids past a static wedge with navier slip and convective boundary conditions. Arab J Sci Eng. 2018. https://doi.org/10.1007/s13369-018-3471-0.